JOURNAL OF MATERIALS SCIENCE: MATERIALS IN MEDICINE 2 (1991) 9–18

Enzymic hydrolysis of biopolymers via single-scission attack pathways: a unified kinetic model

R. AZHARI, N. LOTAN
Department of Biomedical Engineering, Technion–Israel Institute of Technology, Haifa 32000, Israel

A unified analytical model is suggested for describing single-scission attack pathways for enzymic hydrolysis of polymers. This model encompasses the preferred attack degradation, as well as the endo- and exo-type ones. The model is based on kinetic and statistic considerations. It was developed to account for a variety of reaction characteristics, including cases in which the kinetic constants depend upon the chain length of the polymeric substrate. The analytical model provides a dynamic description of the enzymic degradation process, including the overall reaction rate, the time course of the reaction and the array of products obtained throughout the process. These characteristics are shown to be affected, to a large extent, by even minor changes in the probabilities for bond cleavage. The model developed also provides the quantitative evidence for the view that the endo- and exo-type degradation pathways are but particular cases of the general, preferred attack one.

1. Introduction

Enzymic hydrolysis of polymers is a rather complex process. The structure of the polymeric substrate, as well as that of the active site of the enzyme, influence the mode of degradation. Thus, various pathways of degradation have been described in the literature for different combinations of polymers and enzymes [1–10].

In a previous communication [11], we have suggested a new classification scheme and nomenclature for these pathways. Thus, the degradation pathways are divided into two main groups.

1. Single-scission attack group: in these processes, each encounter between enzyme and substrate results in scission of one bond only. This group includes the preferred attack and the endo- and exo-type attack pathways.

2. Multiple-scission attack group: in these processes, each encounter between enzyme and substrate results in scission of more than one bond. For this to be achieved, after the initial scission step, the enzyme remains attached to one of the degradation fragments, and performs a few additional scissions before the enzyme–substrate complex dissociates. This group includes the single-chain attack and the repetitive attack pathways.

In the single-scission group, the preferred attack pathway has already been considered in the literature. For example, the degradation of amylose by α-amylase from *Bacillus amyloliquefaciens* or from *Aspergillus oryzae* [2–4] follows this pathway. It was pointed out that, in such a process, the susceptibility of bonds to enzymic attack depends upon their location in the polymeric chain. This susceptibility can be expressed in terms of probability for cleavage [2–4]. The latter can be calculated using energy maps [2, 4].

The affinity of the enzyme for a macromolecular substrate is often dependent upon the length of the polymeric chain. Kusunoki *et al.* [8] and Pasari *et al.* [9] have shown that for the degradation of glucose oligomers by glucoamylase, the kinetic constants depend upon the length of the oligomeric substrate. We also noted such a dependence when describing the degradation of a synthetic homopolypeptide, poly-*N*-(2-hydroxyethyl)-*L*-glutamine by papain [10, 12–15]. In both cases the enzymes degrade long polymeric chains more readily than the short oligomers. On the other hand, the degradation of low molecular weight inulin by *Kluyveromyces fragilis* inulinase was claimed to be more rapid than that of high molecular weight inulin [16, 17].

In considering the degradation of macromolecular substrates, the multiplicity of possible reaction pathways and the complexity of the process lead to a similarly complex anlaysis. Moreover, in such cases, analytical procedures for interpretation of experimental data, as applied when considering enzymic reactions on low molecular weight substrates, are not always appropriate. Specific models were developed to describe the degradation of a polymer by endo- and exo-type attack [18], by the preferred attack [4, 21] and by the repetitive attack [6, 19–22]. Only some of these models [4, 18] enable prediction of the distribution of degradation products throughout the reaction

0022–2461/91 $03.00 + .12

course. Moreover, most of the models do not account for the dependence of kinetic constants on the chain length of the polymeric substrate.

In this report we present a unified kinetic model for describing the enzymic degradation of polymers via single-scission attack pathways. The suggested model has three unique features:

1. It is capable of accounting for all single-scission attack processes. In this context, the endo- and exo-type attacks are shown to be but particular cases of the general, preferred attack pathway.
2. It takes into consideration dependence of kinetic constants on the chain length of the polymeric substrate.
3. It enables computation of the chain-length distributions of products obtained at any stage of the reaction.

A similar approach was used in deriving analytical models for describing biodegradation processes via multiple-scission attack pathways. These will be considered in a subsequent report.

2. Definitions and assumptions

2.1. The system

The analysis presented below addresses itself to systems in which a soluble, linear (unbranched) homopolymer is hydrolysed by a single enzyme, which acts along a defined degradation pathway.

This analysis can be further extended to include additional kinetic features, such as chain transfer, fragment condensation or enzyme inhibition. It can also be extended to account for degradation of more complex polymeric substrates, such as copolymers. These aspects will be considered elsewhere.

2.2. Kinetic considerations

The analytical model is developed by extending the basic Michaelis–Menten approach. Thus, kinetic expressions describing the concentrations of all species present in the reaction mixture are written, and these are integrated in an overall mass balance. A dynamic description of the entire system is thus obtained.

2.3. Chain-length dependence of kinetic constants

An important feature of the analytical models presented below is that all kinetic constants are taken to be dependent upon the size of the polymeric substrate. Thus, for example, when considering the Michaelis constant, a characteristic value, namely $K_{M,i}$, is assigned for each polymeric chain of length i. Obviously, a system exhibiting a constant K_M is but a particular case of this general situation.

In instances when individual $K_{M,i}$ values are involved, standard experimental procedures for determination of the Michaelis constant can nevertheless be applied. However, in this case, an apparent value, $K_{M,v}$, rather than the individual $K_{M,i}$ values, will be obtained. The quantity $K_{M,v}$ expresses not only the average chain length, v, of the polymeric substrate, but also additional features, such as the actual chain-length distribution of fragments present in the system. The exact correlation between $K_{M,v}$ and $K_{M,i}$ is discussed in detail in Section 3.3.

2.4. Probability considerations

In order to account for the variety of degradation pathways, probability considerations are included in our model.

(a) To each hydrolysable bond in the system, a certain scission probability, $P_{i,j}$, is attributed, expressing the relative susceptibility of the bond to enzymic attack. The index i indicates the total number of residues in the polymeric chain considered, whereas the index j indicates the location of the particular bond in that chain. $P_{i,j}$ values are defined in relative terms, being normalized with respect to the highest probability in the system. Thus, $0 \leq P_{i,j} \leq 1$.

It should be pointed out that, within the context of this paper, the probability for bond scission determines only the site of enzymic attack, whereas the reaction rate is related to the kinetic constants (for details, see Section 3.1).

(b) For each polymeric chain of given size, a unique probability profile is delineated. This profile is made up of the individual $P_{i,j}$ quantities pertaining to the bonds involved. In this study, we limit ourselves to probability profiles in which $P_{i,j}$ is constant for bonds located beyond a certain position from a chain end. For such systems, the characteristic features of the probability profile are: P_{min}, the lowest value of $P_{i,j}$, for a given i; z, the number of hydrolysable bonds, counting from the chain end, beyond which $P_{i,j}$ is independent of j; the highest $P_{i,j}$ in the system. This value is always 1, as defined above; and probability values, intermediate between P_{min} and 1. These were used in calculations, as indicated in Section 3.4 and Table I.

It should be emphasized that the probability profile is not related at all to the origin of the chain it represents. Thus, chains of particular length, whether present from the onset of the process or produced during the process, are all tagged by the same probability profile. Examples of probability profiles, as considered in this study, are shown in Fig. 1.

3. Results

3.1. The preferred attack pathway: analytical model

When a polymer undergoes enzymic degradation, chain fragments containing i residues (i.e. S_i) are formed and consumed simultaneously. The elementary processes involved are:

1. Formation of S_i by enzymic degradation of chains $S_y (y > i)$, via the complex $(ES)_y$

$$E + S_y \underset{k_{2,y}}{\overset{k_{1,y}}{\rightleftharpoons}} (ES)_y \xrightarrow{k_{3,y}} S_i + S_{y-i} + E \quad (1)$$

TABLE I Input parameters to the computer program

Parameter	Symbol[a]	Units
Michaelis constants[b]	$K_{M,i}$ (for $i = 1$ to N)	mM[c]
Catalytic constants[b]	$k_{3,i}$ (for $i = 1$ to N)	min^{-1}
Size of the longest chain present in the system	N	Number of residues
Total concentration of enzyme in the system	C_{ET}	mM
Initial concentration of polymer fragments[b]	$C_i(0)$ (for $i = 1$ to N)	mM[d]
Probabilities for bond cleavage[b]	$P_{i,j}$ (for $i = 1$ to N and $j = 1$ to $i - 1$)	
Molecular weight of a residue		$g\ mol^{-1}$
Duration of the reaction		min
Initial integration step		min
Constant for division of integration step		

[a] As appears in equations in the text.
[b] Defined in terms of a mathematical function, or as discrete values.
[c] Defined in terms of cleavable bonds.
[d] Defined in terms of molecules.

2. Formation and decomposition of complexes $(ES)_i$ between the enzyme and S_i

$$E + S_i \underset{k_{2,i}}{\overset{k_{1,i}}{\rightleftharpoons}} (ES)_i \qquad (2)$$

Thus, the mass balance for polymeric chains of size i is described by

$$\frac{dC_i}{dt} = -k_{1,i}C_E(C_i)_{eff} + k_{2,i}(C_{ES})_i + \sum_{j=i+1}^{N}\left[k_{3,j}\frac{P_{i,j}}{\sum_{l=1}^{j-1}P_{l,j}}(C_{ES})_j\right] + \sum_{j=i+1}^{N}\left[k_{3,j}\frac{P_{j-i,j}}{\sum_{l=1}^{j-1}P_{l,j}}(C_{ES})_j\right] \qquad (3)$$

where C_i is the concentration of chain fragments containing i residues; $(C_i)_{eff}$ is the effective concentration of hydrolysable bonds which are part of chains of length i, and are available to the enzyme at a given point in time. For a more detailed definition, see below; C_E is the concentration of free enzyme; $(C_{ES})_i$, $(C_{ES})_j$ are the concentration of complexes $(ES)_i$ and $(ES)_j$, respectively; N is the number of residues in the longest chain present in the system; $k_{1,i}$, $k_{2,i}$, $k_{3,i}$ are the elementary kinetic constants pertaining to degradation of a polymeric chain of length i (see also Equations 1 and 2). Quantities $k_{1,x}$, $k_{2,x}$, $k_{3,x}$ are similarly defined for any value of x; $P_{i,j}$, $P_{l,j}$ are the probability for cleaving the bond following the ith and lth residues, respectively, from the end of a chain containing j residues.

It should be pointed out that the quantity $(C_i)_{eff}$ does not represent concentration of real species present in solution, but is related to C_i via Equation 4, where $P_{l,i}$ is defined similarly to $P_{i,j}$ and $P_{l,j}$ above

$$(C_i)_{eff} = C_i\sum_{l=1}^{i-1}P_{l,i} \qquad (4)$$

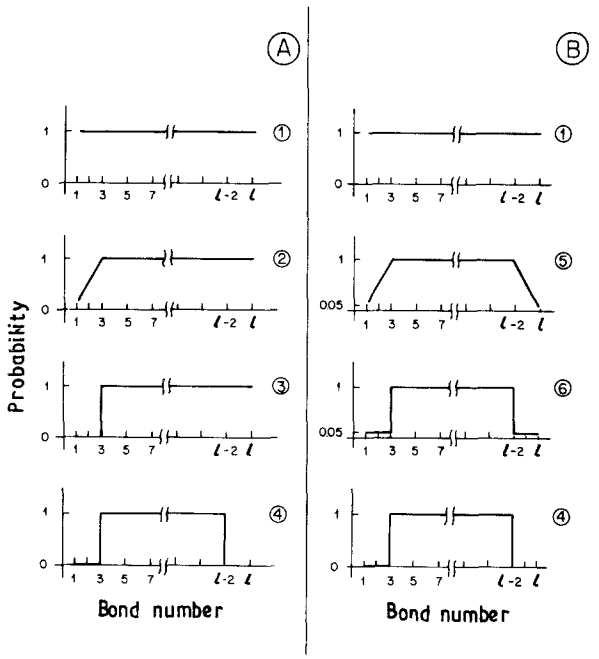

Figure 1 Two groups of probability profiles for enzymic degradation of polymeric chains of l residues, as considered in the present study. For clarity, these profiles are presented as continuous lines, while, as a matter of fact, they are a set of discrete values.

Thus $(C_i)_{eff}$ is a mathematical concept and it accounts for the concentration of substrate which is actually available to the enzyme at a given point in time. This concept takes into consideration the susceptibility of particular bonds to enzymic attack. Particular examples are considered in Section 3.2.

Using Equation 4, the rate of change in concentration of the complex $(ES)_i$ can be described by the mass balance equation

$$\frac{d(C_{ES})_i}{dt} = \left[k_{1,i}C_E C_i\sum_{l=1}^{i-1}P_{l,i}\right] - k_{2,i}(C_{ES})_i - k_{3,i}(C_{ES})_i \qquad (5)$$

Under the quasi-steady-state approximation, Equation 6 holds

$$\frac{d(C_{ES})_i}{dt} = 0 \quad (6)$$

and Equation 5 becomes

$$(C_{ES})_i = \frac{k_{1,i}}{k_{2,i} + k_{3,i}} C_E C_i \sum_{l=1}^{i-1} P_{l,i} \quad (7)$$

Combining Equations 3 and 7, Equation 8 is obtained

$$\frac{dC_i}{dt} = -\left[k_{3,i}\frac{k_{1,i}}{k_{2,i} + k_{3,i}} C_E C_i \sum_{l=1}^{i-1} P_{l,i}\right] + C_E \sum_{j=i+1}^{N}\left[k_{3,j}\frac{k_{1,j}}{k_{2,j} + k_{3,j}} C_j (P_{i,j} + P_{j-i,j})\right] \quad (8)$$

We now refer to the basic definition of the Michaelis constant, $K_{M,x}$, as expressed in Equation 9 for any value of x

$$K_{M,x} = \frac{k_{2,x} + k_{3,x}}{k_{1,x}} \quad (9)$$

Using this definition, Equation 8 can be rewritten as Equation 10

$$\frac{dC_i}{dt} = -\left[\frac{k_{3,i}}{K_{M,i}} C_E C_i \sum_{l=1}^{i-1} P_{l,i}\right] + C_E \sum_{j=i+1}^{N}\left[\frac{k_{3,j}}{K_{M,j}} C_j (P_{i,j} + P_{j-i,j})\right] \quad (10)$$

For use in this equation, the quantity C_E is calculated from the mass balance on the enzyme in the entire system. Thus

$$C_E = C_{ET} - \sum_{j=2}^{N} (C_{ES})_j = C_{ET} - \sum_{j=2}^{N}\left(\frac{1}{K_{M,j}} C_E C_j \sum_{l=1}^{j-1} P_{l,j}\right) \quad (11)$$

where C_{ET} is the total concentration of enzyme, and $(C_{ES})_j$ is taken from an expression similar to Equation 7, after interchanging i and j.

The concentration of free enzyme is, then, given by the equation

$$C_E = \frac{C_{ET}}{\left[1 + \sum_{j=2}^{N}\left(\frac{1}{K_{M,j}} C_j \sum_{l=1}^{j-1} P_{l,j}\right)\right]} \quad (12)$$

It should be noted that Equation 10 actually represents a set of N ordinary differential equations, each being related to a certain chain length, i. This set of equations can be solved numerically, to yield the chain length distribution of fragments present in the system at any stage of the degradation process.

3.2. Single-scission attack pathways: a unified view

The models developed above lead to a unified view of the single-scission attack pathways. This is attained by introducing two new concepts: probability profile (defined in Section 2.4), and effective concentration (defined in Equation 4). Relying on these concepts, and using appropriate values for the parameters involved, the mathematical description of any particular single-scission attack pathway can be achieved, as shown below.

In terms of this unified approach, let us consider the two pathways most frequently encountered during enzymic attack of polymers: the endo- and exo-type attack.

In the endo-type attack, each of the $(i-1)$ bonds in the chain is equally susceptible to enzymic attack, and contributes equally to the effective substrate concentration. Thus, in this case, $(C_i)_{eff}$ is also the total concentration of hydrolysable bonds in the system.

In the exo-type attack, at any given moment there is only one site for enzymic attack on each chain, namely the chain end. Hence, in this case, $(C_i)_{eff}$ is the total concentration of polymeric molecules of length i.

This view can now be examined quantitatively, using the analytical model developed above, and implementing the conditions prevailing in the system during endo- or exo-type attack.

3.2.1. A particular case: the endo-type attack

In this case, Equation 13 holds for all values of i and j

$$P_{i,j} = 1 \quad (13)$$

Combining Equations 10 and 13, one obtains

$$\frac{dC_i}{dt} = -\frac{k_{3,i}}{K_{M,i}} C_E C_i (i - 1) + 2C_E \sum_{j=i+1}^{N}\left(\frac{k_{3,j}}{K_{M,j}} C_j\right) \quad (14)$$

Also, combining Equations 12 and 13, one obtains

$$C_E = C_{ET} \Big/ \left\{1 + \sum_{j=2}^{N}\left[\frac{1}{K_{M,j}} C_j (j - 1)\right]\right\} \quad (15)$$

As indicated above for Equation 10, Equation 14 also represents an entire set of differential equations, each for a given chain length. This set, as well as Equation 15, are actually more general forms of the equations described by Suga *et al.* [18]. The latter were developed for the particular case of the endo-type attack pattern, and do not allow for the possibility that the kinetic constants might be dependent upon the size of the polymeric substrate.

The fact that the endo-type attack can be considered as a particular case of the preferred-attack pathway is also substantiated by the results of numerical simulations. These are presented in Section 3.5 below.

3.2.2. A particular case: the exo-type attack

The two ends of a biopolymer chain differ from one another, e.g. reducing and non-reducing ends in a polysaccharide molecule, or amino- and carboxy-termini in a polypeptide molecule. Owing to specificity

of their action, exo-type enzymes degrade polymeric chains by cleaving fragments (usually monomers) from one end of the molecule only. Thus, when expressed in terms of probabilities for cleavage, as these appear in Equation 10, the exo-type degradation is characterized by

$$\left.\begin{array}{ll} \text{for } l = 1 & P_{l,i} = 1 \\ \text{for } l \neq 1 & P_{l,i} = 0 \\ \text{for } i = 1 & P_{i,j} = 1 \\ \text{for } i \neq 1 & P_{i,j} = 0 \\ \text{for } j - i = 1 & P_{j-i,j} = 1 \\ \text{for } j - i \neq 1 & P_{j-i,j} = 0 \end{array}\right\} \quad (16)$$

Using these probability values, Equation 10 becomes

for $i \neq 1$

$$\frac{dC_i}{dt} = -\frac{k_{3,i}}{K_{M,i}} C_i C_E + \frac{k_{3,i+1}}{K_{M,i+1}} C_{i+1} C_E \quad (17)$$

for $i = 1$

$$\frac{dC_1}{dt} = \left(\sum_{j=3}^{N} \frac{k_{3,j}}{K_{M,j}} C_j C_E\right) + 2\frac{k_{3,2}}{K_{M,2}} C_2 C_E \quad (18)$$

Also, for the probability values shown in Equation 16, Equation 12, expressing the concentration of free enzyme, now becomes

$$C_E = C_{ET} \Big/ \left[1 + \sum_{j=2}^{N} \left(\frac{1}{K_{M,j}} C_j\right)\right] \quad (19)$$

Similar to what is indicated for Equations 14 and 15, Equation 17 also represents an entire set of differential equations, each for a given chain length. This set together with Equations 18 and 19, are actually more general forms of the equations described by Suga *et al.* [18]. The latter were developed for the particular case of the exo-type attack pattern, and do not allow for the possibility that the kinetic constants might be dependent upon the size of the polymeric substrate.

3.3. Correlation between $K_{M,v}$ and $K_{M,i}$

As mentioned in Section 2.3, in instances when individual $K_{M,i}$ values are involved, interpretation of experimental data in terms of standard procedures leads to an apparent value, $K_{M,v}$, rather than to the individual $K_{M,i}$ values. In this section, the correlation between these quantities is deduced.

When an enzyme degrades a polymer via the single-scission attack pathway, the total rate of reaction can be described by Equation 20

$$V = \sum_{i=1}^{N} \frac{dC_i}{dt} \quad (20)$$

Combining Equations 10 and 20, we obtain

$$V = -\sum_{i=1}^{N}\left[\frac{k_{3,i}}{K_{M,i}} C_E C_i \sum_{l=1}^{i-1} P_{l,i}\right] + C_E \sum_{i=1}^{N}\left\{\sum_{j=i+1}^{N}\left[\frac{k_{3,j}}{K_{M,j}} C_j (P_{i,j} + P_{j-i,j})\right]\right\} \quad (21)$$

Rearranging Equation 21, Equation 22 is obtained

$$V = C_E \sum_{i=2}^{N}\left(\frac{k_{3,i}}{K_{M,i}} C_i \sum_{j=1}^{i-1} P_{j,i}\right) \quad (22)$$

Inserting the expression for C_E from Equation 12, Equation 22 becomes

$$V = \frac{C_{ET} \sum_{i=2}^{N}\left(\frac{k_{3,i}}{K_{M,i}} C_i \sum_{j=1}^{i-1} P_{j,i}\right)}{1 + \sum_{i=2}^{N}\left(\frac{1}{K_{M,i}} C_i \sum_{j=1}^{i-1} P_{j,i}\right)} \quad (23)$$

For examplification on how Equation 23 is utilized, we here consider the particular case in which the catalytic constant is independent of the length of the polymeric substrate (i.e. $k_{3,i} = k_3$). Under these conditions Equation 23 becomes

$$V = \frac{k_3 C_{ET} \sum_{i=2}^{N}\left(\frac{1}{K_{M,i}} C_i \sum_{j=1}^{i-1} P_{j,i}\right)}{1 + \sum_{i=2}^{N}\left(\frac{1}{K_{M,i}} C_i \sum_{j=1}^{i-1} P_{j,i}\right)} \quad (24)$$

We note that

$$k_3 C_{ET} = V_{max} \quad (25)$$

and Equation 24 can thus be rewritten in terms of V_{max}

$$V = \frac{V_{max} \sum_{i=2}^{N}\left[\frac{1}{K_{M,i}} C_i \sum_{j=1}^{i-1} P_{j,i}\right]}{1 + \sum_{i=2}^{N}\left[\frac{1}{K_{M,i}} C_i \sum_{j=1}^{i-1} P_{j,i}\right]} \quad (26)$$

Equation 25 expresses the reaction rate using individual parameters for each size polymer. However, when considering only the average chain length of the polymer (v), the reaction rate must be redefined. This is done in Equation 27 in terms of V^*, and using Equation 25

$$V^* = \frac{V_{max} C_v (v - 1)}{K_{M,v} + C_v (v - 1)} \quad (27)$$

In this equation, the factor $(v - 1)$ is included so that concentration of actual substrate (i.e. hydrolysable bonds) be related to the apparent concentration of molecules of size v (i.e. C_v). We also consider the definitions of v (Equation 28) and C_v (Equation 29)

$$v = \frac{\sum_{i=1}^{N} i C_i}{\sum_{i=1}^{N} C_i} \quad (28)$$

$$C_v = \sum_{i=1}^{N} C_i \quad (29)$$

Using these definitions, Equation 27 becomes

$$V^* = \frac{V_{max} \sum_{i=1}^{N} C_i (i - 1)}{K_{M,v} + \sum_{i=1}^{N} C_i (i - 1)} \quad (30)$$

Considering the fact that the observed rate of reaction is an experimental quantity, it does not depend on the

mode of interpretation of the results. It, therefore, necessarily follows that

$$V = V^* \tag{31}$$

and from Equations 26, 30 and 31, we obtain

$$\frac{V_{max}\sum_{i=2}^{N}\left[(1/K_{M,i})C_i\sum_{j=1}^{i-1}P_{j,i}\right]}{1+\sum_{i=2}^{N}\left[(1/K_{M,i})C_i\sum_{j=1}^{i-1}P_{j,i}\right]} = \frac{V_{max}\sum_{i=1}^{N}C_i(i-1)}{K_{M,v}+\sum_{i=1}^{N}C_i(i-1)} \tag{32}$$

Equation 32 leads to the correlation between $K_{M,v}$ and $K_{M,i}$

$$K_{M,v} = \frac{\sum_{i=2}^{N}C_i(i-1)}{\sum_{i=1}^{N}(1/K_{M,i})C_i\sum_{j=1}^{i-1}P_{j,i}} \tag{33}$$

It can be seen that $K_{M,v}$ expresses the actual chain-length distribution of fragments present in the system, as well as the probabilities for bond cleavage.

As indicated above, Equation 33 was derived for the particular case when, for all values of i, $k_{3,i} = k_3$. When this limitation is not applicable, correlations similar to that shown in Equation 33 can also be obtained, and this is achieved starting from Equation 23 rather than Equation 24.

3.4. Computation procedures

It was mentioned above that the analytical models developed lead to a set of ordinary differential equations, each describing the change in concentration of a polymeric chain of given length. These equations can be solved numerically. To this aim a computer program was written, and is based on the Euler method [23]. This method is very sensitive to the size of the integration step. Therefore, a mass balance on the total number of residues in the system is included in the program, and the integration step is selected as the largest one which satisfies the mass balance (within 0.1%).

The input parameters required by the computer program are listed in Table I. We note that amongst them, the ones related to the molecular size of the polymeric substrate, i, can be supplied either as a chosen mathematical function of i, or as a chosen set of discrete values. The input list also includes parameters related to the integration steps utilized for numerically solving the differential equations. These parameters are required because stability errors, intrinsic to the Euler method employed, may occur. In this study, we utilize the residue mass balance as a guide for choosing appropriate values of the above parameters.

The output data are listed in Table II. As can be seen, using the procedures developed, a dynamic description of the degradation process is thus obtained. It is expressed merely in terms of the chain length distribution of degradation fragments, as produced at each stage of the reaction. This distribution is the basic information, from which many physical characteristics of the system can now be deduced. For example, the number- and weight-average molecular weights, polydispersity, as well as hydrodynamic and thermodynamic properties can be calculated.

In principle, one can also conceive the inverse mode of utilization of the analysis presented herein, namely to combine detailed experimental data with the kinetic models and computer program developed, in order to delineate analytical expressions for $K_{M,i}$, $k_{3,i}$ and/or $P_{i,j}$ functions. This possibility is not yet included in the computer program developed. For this to be achieved, curve fitting and parameter estimation subroutines must also be included.

3.5. Results of numerical simulations

The models described above were used to simulate the time course of a variety of polymer degradation processes. Thus, degradation by endo- and exo-type enzymes, as well as the effect of initial distribution of polymer chain lengths were considered in previous reports [13, 14]. In this report we present an extensive analysis on the correlation between the detailed

TABLE II Data output from the computer program

Parameter	Symbol[a]	Units
Concentration of degradation products at any given time, t	C_i (for i = 1 to N)	mM[b]
Mass balance on residues in the system at any given time, t		[c]
Total concentration of bonds cleaved, from the onset of the reaction till time, t		mM[d]
Optional		
Extent of reaction		% hydrolysis
Average chain length	v	Number of residues
Number average molecular weight		g mol^{-1}
Weight average molecular weight		g mol^{-1}
Polydispersity		
Weighted-average Michaelis constant[e]	$K_{M,v}$	mM[d]

[a] As appears in equations in the text.
[b] Defined in terms of molecules.
[c] Expressed in terms of % discrepancy relative to the initial total concentration of residues in the system.
[d] Defined in terms of bonds.
[e] See Sections 2.3 and 3.3.

characteristics of the probability profile, on the one hand, and the size distribution of degradation products and its change during the reaction, on the other hand.

3.5.1. General case: the preferred attack pathway

The probability profiles utilized in this study are shown in Fig. 1. As can be seen, two groups, A and B, were considered. In each group, profiles were varied in a systematic manner, so that effects of each variation can be analysed in all its details. Thus, in both groups, we started from a probability profile characteristic to a strictly random attack (profile 1), and ended with one in which the bonds adjacent to the chain ends are completely stable to enzymic attack (profile 4). However, the intermediate profiles differ from one group to the other.

Probability profiles, as shown in Fig. 1, can indeed be encountered in actual experimental cases. For example, profile 1 is characteristic of degradation by an endo-type enzyme, while profile 3 is pertinent to degradation of a polyaminoacid by carboxypeptidase.

Results of numerical simulation are presented below, in terms of extent of reaction (Fig. 2), and size distribution of degradation fragments (Figs 3 and 4). In each case, the pertinent probability profile is indicated in the figure, while for the other parameters involved, numerical values employed in calculations are collected in Table III.

From the results presented it can be clearly seen that even very small differences in the probability profiles (particularly in the susceptibility to cleavage of bonds at polymer ends) may have considerable effects on the degradation process. These effects are expressed not only in the extent of the reaction, but in the composition of products as well.

The effects of P_{min} (for a constant value of z) were investigated in detail for probability profile 6. The results obtained are shown in Figs 5 and 6. We note that the most pronounced effects are seen at low values of P_{min}, namely $0 < P_{min} < 0.1$, and this is true both for extent of degradation (Fig. 5) and molecular size distribution of products (Fig. 6).

The effect of changing z, for a constant value of P_{min}, was also investigated in this study. Thus, for

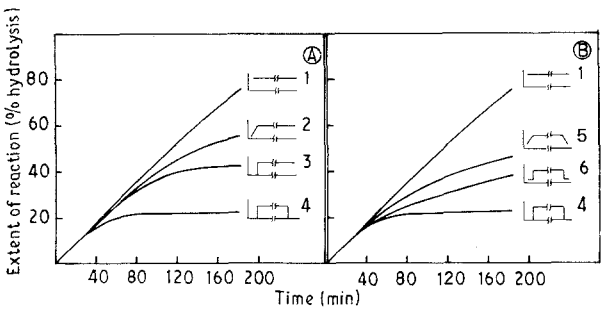

Figure 2 Effect of probability profile on the time course of the degradation reaction. The probability profile considered in each calculation is schematically indicated near the corresponding curve, and shown in detail in Fig. 1. For numerical values of other parameters used in the simulations, see Table III.

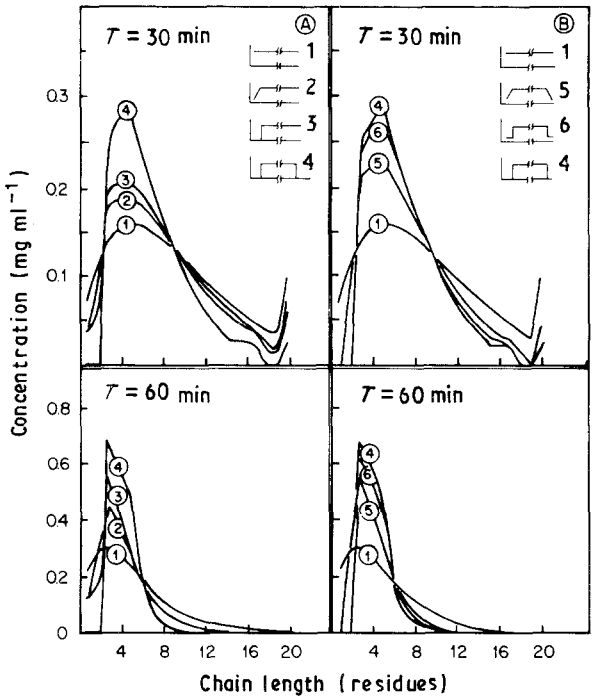

Figure 3 Size distribution of fragments obtained 30 and 60 min after the onset of the degradation reaction. The probability profiles considered in the calculations are schematically indicated, and the concentration profiles are marked accordingly. The probability profiles are shown in detail in Fig. 1. For numerical values of other parameters used in the simulations, see Table III.

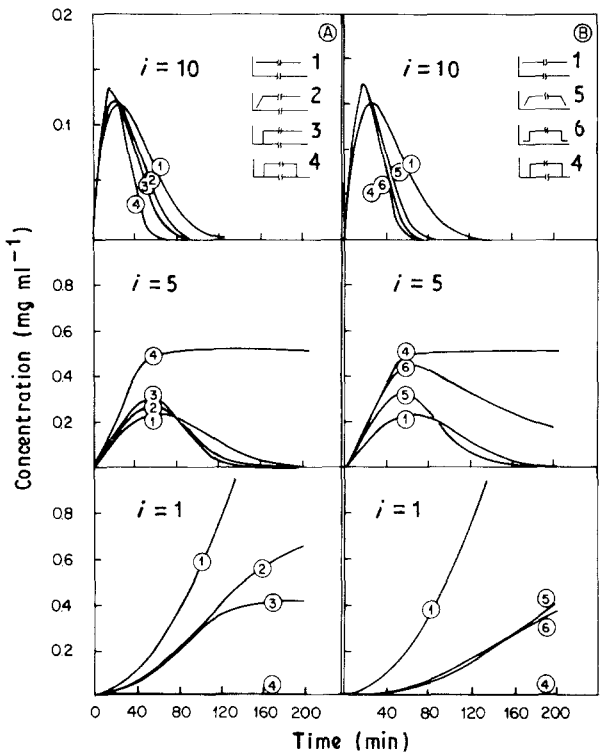

Figure 4 Dynamic description of the concentration of fragments of various sizes, i, during the degradation reaction. The probability profiles considered in the calculations are schematically indicated, and the concentration profiles are marked accordingly. The probability profiles are shown in detail in Fig. 1. For numerical values of other parameters used in the simulations, see Table III.

systems characterized by probability profile 6, results are shown in Figs 7 and 8. We note that z determines, to a large extent, the time course of the reaction (Fig. 7) as well as the molecular size distribution of products (Fig. 8).

TABLE III Numerical values for the parameters employed in computation of data presented in Figs 2, 3 and 4

Parameter	Symbol[a]	Value	Units
Michaelis constant	$K_{M,i}$ (for i = 1 to N)	2	mM[b]
Catalytic constant	$k_{3,i}$ (for i = 1 to N)	1	min^{-1}
Size of the longest chain present in the system	N	20	Number of residues
Total concentration of enzyme in the system	C_{ET}	0.1	mM
Initial concentration of polymer fragments	$C_i(0)$		
	for i = 1 to 19	0	mM[c]
	for i = 20	1	mM[c]
Probabilities for bond cleavage	$P_{i,j}$	[d]	
Molecular weight of a residue in the polymeric chain		180	$g\ mol^{-1}$
Duration of the reaction		240	min
Initial integration step		1	min
Constant for division of integration step		2	

[a] As appears in equations in the text.
[b] Defined in terms of bonds.
[c] Defined in terms of molecules.
[d] As indicated in each figure. For details see also Fig. 1.

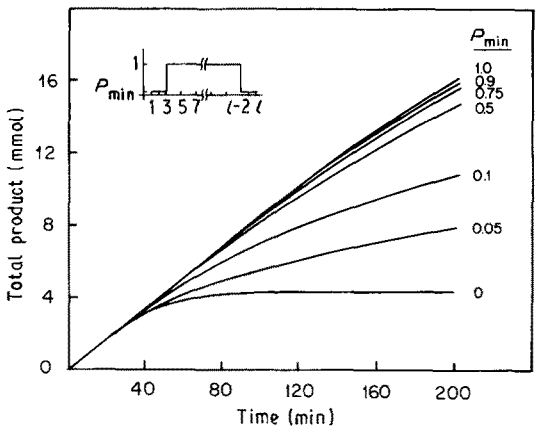

Figure 5 Effect of P_{min} on the time course of the degradation reaction. The probability profile considered in calculations (probability profile 6 in Fig. 1) is schematically indicated. Numerical values of other parameters used in the simulations are collected in Table III.

3.5.2. A particular case: the endo-type attack

The view that endo-type attack is a particular case of the preferred attack degradation pathway was deduced on analytical grounds, as indicated in Section 3.2.1 above. This is also clearly seen from results of numerical simulations. Thus we note that this limiting case is reached when $P_{min} = 1$ (Fig. 5) or when $z = 1$ (Fig. 7). Moreover, these models were used for analysing the degradation of a homopolymer, poly-*N*-(hydroxyethyl)-*L*-glutamine (PHEG), by papain, an enzyme known to be of the endo-type. Good agreement was reached between theoretical and experimental results [13, 14].

3.5.3. A particular case: the exo-type attack

The view that exo-type attack is a particular case of the preferred attack degradation pathway was also deduced on analytical grounds, as indicated in Section

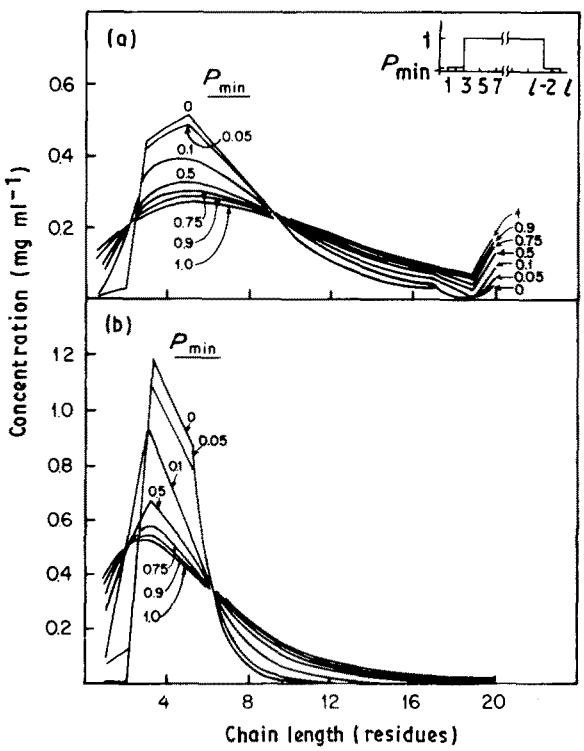

Figure 6 Effect of P_{min} on the size distribution of fragments obtained 30 and 60 min after the onset of the degradation reaction (panels (a) and (b) respectively). The probability profile considered in calculations (probability profile 6 in Fig. 1) is schematically indicated. Numerical values of other parameters used in the simulations are collected in Table III.

3.2.2 above. Using this approach, numerical simulations were performed to assess the effect of the kinetic parameters on the time course of the degradation process. The results obtained were reported previously [13, 14].

4. Discussion

In a previous report [11], mechanistic aspects concerning polymer degradation by enzymes were considered. In particular, a unified view was presented

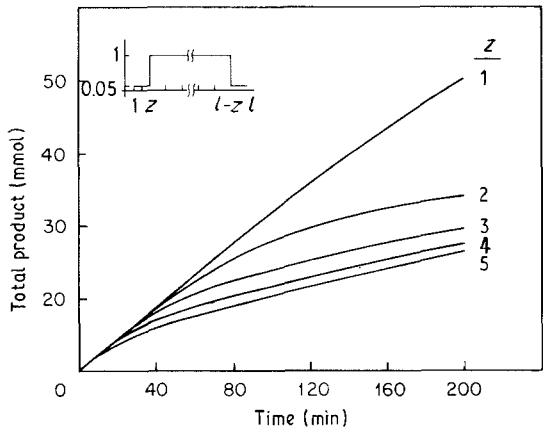

Figure 7 Effect of z on the time course of the degradation reaction. The probability profile considered in calculations (probability profile 6 in Fig. 1) is schematically indicated. Numerical values of other parameters used in the simulations are collected in Table III.

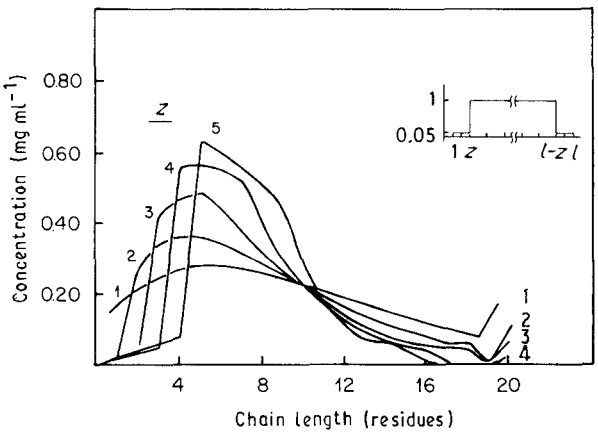

Figure 8 Effect of z on the size distribution of fragments obtained 30 min after the onset of the degradation reaction. The probability profile considered in calculations (probability profile 6 in Fig. 1) is schematically indicated. Numerical values of other parameters used in the simulations are collected in Table III.

regarding all degradation patterns along which an effective encounter between enzyme and its polymeric substrate leads to scission of one bond only. This unified view, the "single-scission attack", thus encompasses the endo- and exo-type degradations. Based on this understanding, a new classification and nomenclature for various enzymic depolymerization processes was offered [11].

In the present report, the analytical basis underlying the above concept is presented. In developing the corresponding kinetic model, the actual size (namely, number of residues, i) of the polymeric substrate is explicitly taken into account. This feature allows us to consider the susceptibility to cleavage of a particular bond when part of polymeric fragments of various sizes. Such a characteristic was encountered when interpreting experimental results, regarding, for example, the Michaelis constant, K_M, for the systems poly-*N*-(hydroxyethyl)-*L*-glutamine (PHEG)-papain [10, 13] and amylose-glucoamylase [8, 9].

The delineation of the single-scission mode of action relies on two concepts.

(a) Effective substrate concentration, $(C_i)_{eff}$. This quantity expresses the actual concentration of available substrate of size i. It should be emphasized that it does not represent concentration of real species in the system, but is a characteristic analogous to the concept of thermodynamic activity. Moreover, this is a weighted quantity and originates in the fact that the substrate is macromolecular and polydisperse with respect to its molecular size.

(b) Probability profiles. They attribute a certain probability for cleavage to each bond in a polymeric chain. In the analytical model we assume that the probability profile is identical for all chains of given size, independent of their origin. Such probability profiles were also derived for the system amylose-α-amylase [2, 4]. In the latter case, energy balance was used in calculations, whereas in our model mechanistic considerations (manifested in mass balances) are applied.

Using the analytical models developed, calculations were performed to simulate enzymic degradation of biopolymers. Particular consideration was given to the dynamic aspects of the processes, and to a detailed description of degradation pathways and size distribution of degradation products. The results obtained (e.g. Figs 5–8), point to the fact that the detailed features of the probability profile have a significant effect on the time course of the degradation and the range of products obtained.

The analytical models established and the results of calculations also provide the quantitative ground for our view that the endo-type attack is a limiting case of the general, preferred-attack, mode of polymer degradation by enzymes. This is clearly seen when considering data presented in Figs 2–4. By analogy, similar evidence can be offered to show that the exo-type attack is also a limiting case of the preferred-attack mode of action (results not shown).

It should be emphasized that the kinetic–statistic analysis presented above, as well as the mathematical models and numerical simulations, are concerned uniquely with single-enzyme degradation of homopolymers. Yet, extension of these studies can be envisaged so as to consider degradation of copolymeric substrates. In such cases, however, it will be necessary to take into account that probability profiles are also determined by the primary structure, i.e. residues sequence, of the polymeric substrate. Fragments obtained during the degradation retain the original sequence and therefore, different probability profiles will have to be attributed to chains which contain the same number of residues, but differ from one another with respect to their primary structure.

The models presented can also be extended to processes involving a few enzymes operating in parallel or in a synergistic manner, and to more complex kinetic mechanisms including enzyme inhibition or chain transfer phenomena. These will be considered in further studies.

Acknowledgements

Partial financial support for this research was provided by the MEP Group of the Women's Division of the American Technion Society, New York, NY, the

Tess Heffner Research Grant, and the Julia Tal Equipment and Research Fund. All are gratefully acknowledged. This study forms part of the DSC thesis of R. Azhari, Technion (1988).

References

1. L. ZITTAN, *Starch* **33** (1981) 373.
2. J. A. THOMA, J. G. SPRADLIN and S. DYGART, in "The Enzymes", edited by P. D. Boyer (Academic Press, New York, London, 1971) p. 115.
3. J. D. ALLEN and J. A. THOMA, *Biochem.* **17** (1978) 2338.
4. J. D. ALLEN, *Methods Enzymol.* **64** (1980) 248.
5. J. F. ROBYT and D. FRENCH, *Arch. Biochem. Biophys.* **122** (1967) 8.
6. J. F. ROBYT, in "Starch: Chemistry and Technology", edited by R. L. Whistler, J. N. Bemiller and E. F. Paschall (Academic Press, New York, London, 1984) p. 87.
7. B. H. NAHM and S. M. BYUN, *Korean Biochem. J.* **10** (2) (1977) 95.
8. K. KUSUNOKI, K. KAWAKAMI, F. SHIRAISHI, K. KATO and M. KAI, *Biotechnol. Bioengng.* **24** (1982) 347.
9. A. J. PASARI, R. A. KORUS and R. C. HEIMSCH, *Enzyme Microb. Technol.* **10** (1988) 156.
10. Y. YAACOBI, N. LOTAN and S. SIDEMAN, *Life Support Systems* **3** (1985) 313.
11. R. AZHARI and N. LOTAN, Journal of Materials Science Letters, in press.
12. Y. YAACOBI, DSc thesis, Technion, Israel Institute of Technology, Haifa, Israel (1985).
13. R. AZHARI and N. LOTAN, *Makromol. Chem. Macromol. Symp.* **19** (1988) 295.
14. R. AZHARI and N. LOTAN, in "Proceedings of the 4th Mediterranean Conference on Medical and Biological Engineering", Sevilla, Spain 1986, edited by L. M. Roa and J. R. Zaragoza (Puntex, Barcelona, 1986) p. 440.
15. R. AZHARI, DSc thesis, Technion, Israel Institute of Technology, Haifa, Israel (1989).
16. W. E. WORKMAN and D. F. DAY, *Biotechnol. Bioengng.* **26** (1984) 905.
17. S. M. BYUN and B. H. NAHM, *J. Food Sci.* **43** (1978) 1871.
18. K. SUGA, G. VAN DADEM and M. MOO-YOUNG, *Biotechnol. Bioengng.* **17** (1975) 433.
19. J. A. THOMA, *Biopolymers* **1** (1976) 729.
20. W. BANKS and C. T. GREENWOOD, *Carbohyd. Res.* **57** (1977) 301.
21. A. K. MAZUR, *Biopolymers* **23** (1984) 859.
22. *Idem, ibid.* **23** (1984) 1735.
23. M. J. MARON, "Numerical Analysis: A Practical Approach" (Macmillan, New York, 1982) p. 337.

Received 10 October 1989
and accepted 31 August 1990